11th International Symposium on Turbulence and Shear Flow Phenomena (TSFP11)
Southampton, UK, July 30 to August 2, 2019

VORTICITY STATISTICS AND DISTRIBUTIONS IN DRAG REDUCED TURBULENT PIPE FLOW WITH TRANSVERSE WALL OSCILLATIONS

Daniel Coxe
School for Engineering of Matter, Transport and Energy (SEMTE)
Arizona State University (ASU)
Address
email

Yulia Peet
SEMTE
ASU
ypeet@asu.edu

Ronald Adrian
SEMTE
ASU
rjadrian@asu.edu

ABSTRACT

Presented are vorticity statistics in drag reduced turbulent pipe flow at low and moderate Reynolds number. Drag reduction is achieved by transverse wall oscillations. Quantities of interest are the distributions of streamwise vorticity in the viscous and lower part of the buffer layer of the flow. We observe a sinusoidal pattern appearing in the distribution that is associated with the strengthening and weakening of counter-rotating vortex pairs. Presented alongside the phase varying distributions of vorticity are the phase averaged distribution of azimuthal and radial velocity fluctuations. The information presented provides a statistical evidence for the new proposed model for the near wall vortex distortion.

1 Introduction

It is well known that wall oscillations in boundary layer, channel, and pipe flow reduce drag (Baron & Quadrio (1995), Choi *et al.* (2002), Duggleby *et al.* (2007)). However, the efficacy of the principle with increasing Reynolds number is not generally established. The majority of research has been focused on low Reynolds number channel flow in the regime of $Re_\tau = \frac{u_\tau R}{\nu} < 200$ (Choi *et al.* (2002); Zhou & Ball (2008); Quadrio *et al.* (2009)). The experiments of Choi & Graham (1998) reported the measurements of bulk drag reduction in turbulent pipe flows with wall oscillation at $Re_\tau = 660$ and 970 but provided no insight into the structure of turbulence.

This work seeks to establish the fundamental mechanisms by which transverse wall oscillations reduce drag in a pipe flow. Our working hypothesis is that quasi-streamwise (QS) buffer layer vortices are sheared by wall oscillations: clockwise pipe rotation applies a torque that increases the vorticity of clockwise rotating QS vortices and decreases the vorticity of counter-clockwise QS vortices, and vice versa. Subsequently, this skewing affects the generation of hairpin vortices above the buffer layer. The strengthening and weakening of opposite-signed QS vortices modifies the direction of momentum transfer by azimuthally tilting the upflow induced between the pairs of QS vortices, thereby reducing the wall normal velocity component and introducing a circumferential component. This distortion has the effect of inhibiting hairpin auto generation.

2 Method

Drag reduction of turbulent pipe flow is explored through a direct numerical simulation at low ($Re_\tau = \frac{u_\tau R}{\nu} = 170$) and moderate ($Re_\tau = 360$) Reynolds number. u_τ is the friction velocity, ν is kinematic viscosity, and R is the pipe radius. The pipe is $24R$ long with a periodic inlet and outlet conditions where the length was chosen to allow for decorrelation of the turbulent fluctuations in the streamwise direction over half the length of the pipe (Guala *et al.* (2006)). The flow is driven by a constant forcing term in the streamwise direction equivalent to a mean pressure gradient in order to better represent a pump driven flow relevant to realistic applications. The solver used is Nek5000, an open source Spectral Element Method code that achieves exponential accuracy with p-refinement (Fischer (1997), Deville *et al.* (2002)). The two meshes were generated such that 5 gridpoints were located below $y^+ = 1$, an average streamwise grid spacing was 8.5 plus units apart for both simulations, with 36 million grid points for $Re_\tau = 170$ and 174 million for $Re_\tau = 360$.

Drag reduction is achieved by means of transverse (azimuthal) wall oscillation modeled by introducing a time-dependent azimuthal wall velocity $u_{\theta\,wall}(t)$, invariant in the streamwise direction, but sinusoidal in time.

Standard cylindrical notation is used for radial, azimuthal and axial components of position (r,θ,x) and velocity (u_r,u_θ,u_x). It is sometimes convenient to employ (x,y,z) and (u,v,w) notation where x is axial, $y = R - r$ is normal to the wall and z is azimuthal. Superscript $+$ denotes non-dimensionalization by the viscous length scale and the mean friction velocity based on the constant mean wall shear stress $\overline{\tau}_{wall} = \langle \tau_{wall}(x,\theta,t)\rangle_{x,\theta,t}$. The azimuthal

wall velocity is given by

$$u^+_{\theta wall}(t^+) = u^+_{wall}\sin(\phi); \phi = \frac{2\pi}{T^+_{osc}}t^+, \qquad (1)$$

where the amplitude $u^+_{wall} = 10$, and the period $T^+_{osc} = 100$ (plus denotes wall units) were chosen in accordance with the previous literature identifying these values as near-optimum for drag reduction (Quadrio & Sibilla, 2000; Quadrio & Ricco, 2004; Quadrio *et al.*, 2009).

Phase averaging is performed to study the effect on statistics within the oscillation cycle. The phase average is denoted by $\langle \mathbf{u}(r)|\phi\rangle_{x,\theta}$, where ϕ is the phase angle of the wall oscillation cycle.

3 Overview of the drag Reduction

The mean drag reduced streamwise velocity (which is azimuthally, axially and temporally averaged but is radially-varying) shown in Figure 1 indicates a substantive increase in both the buffer layer ($0 < y^+ < 30$) and the outer flow ($30 < y^+ < Re_\tau$) for the drag reduced pipe showing that wall oscillations affect the QS eddies in the buffer layer and the hairpin eddies that form above it. Correspondingly, the mean Reynolds stress $\langle u'_x u'_r\rangle_{x,\theta,t}$ shown in the same figure is also reduced in and above the buffer layer. The net drag reduction achieved in the current study is 37% for $Re_\tau = 170$, and 36% for $Re_\tau = 360$.

4 Proposed Model

The motivation of this paper is to propose a model of the effects of a wall oscillation on the near wall vortices and the resulting induced fluctuating field. The model is presented in this section and the statistical evidence to support the model will follow in the subsequent sections. The model seeks to present a qualitative explanation for a decreased momentum transfer from the near wall to the bulk. We assert that due to the wall oscillations, counter-rotating vortex pairs are made significantly unequal such that momentum transfer is skewed into transverse directions. Given the distributions presented in Sections 5, 6 as a function of phase, the proposed model of drag reduction is illustrated in Figure 2.

Starting from the beginning of the wall oscillation cycle illustrated in the top figure ($\phi = 0$, ϕ is the wall velocity phase angle, see Eq. (1)), the flow has just experienced half a period of negative wall velocity which acts to strengthen the clockwise vortices. As the wall oscillations progress, somewhere in the first quarter phase, the streamwise vortices are returned to equal strength for pairs of counter-rotating vortices. However as the wall continues to move in the positive transverse direction, the counterclockwise vortical structures are enhanced skewing ejection and sweep events and thus reducing momentum transfer between the bulk and the wall region. The second half the of the wall oscillation is simply a mirror image of the first half where induced velocities are skewed in opposite directions.

5 Vorticity Distributions

In this section we present the premultiplied distributions of vorticity to illuminate the effects of the wall oscillations on the distribution of vorticity at select wall distances. Coordinates of $y^+ = 10, 20,$ and 30 are chosen to illustrate how the streamwise vorticity in these regions are enhanced by the wall oscillations because it is in these regions that ejection events are most relevant to drag.

5.1 Long term Average Distribution of Vorticity

Presented are the distributions of streamwise vorticity at three y^+ coordinates at both Reynolds numbers. Figures 3 through 5 show the distributions for $Re_\tau = 170$, while Figures 6 through 8 illustrate the same distributions for the $Re_\tau = 360$ case. Overall the weighted distribution has been *pushed out* indicating that large streamwise vortices occur with higher frequency. This comes as a result of wall oscillations imparting a spanwise momentum thus increasing the likelihood of large amplitude vortices. From Figures 3-8, it can be seen that through the buffer layer the width of the distributions are 10% to 50% wider at any given y^+. The phase variation of these fluctuations will later be shown to track the wall oscillations.

The broadened streamwise vorticity distributions associated with the wall oscillations indicate that the wall oscillations increase the streamwise vorticity variance. The streamwise vorticity variance for the two Reynolds numbers and the wall locations of $y^+ = 10, 20, 30$ and 44 is tabulated in Table 1. Indeed, an increase in variance is noticed for the oscillated versus standard pipe for all presented wall locations and both Reynolds numbers, albeit the effect is diminished with the distance from the wall and is slightly smaller at higher Reynolds number.

5.2 Phase Varying Distributions

In order to understand the inherently temporal behavior of the flow, it is necessary to view the flow as a function of a wall phase. Applying the triple decomposition mechanism as in Hussain & Reynolds (1970) we can look at the phase dependence of fluctuation distributions. Figures 9 through 14 present the pre-multiplied streamwise vorticity distributions over the wall phase angle. Color contours are of the pre-multiplied probability density function of the streamwise vorticity. The x-axis indicates the wall velocity phase angle and the y-coordinate is the value of the streamwise vorticity.

At the start of the wall oscillation, the vorticity in the region around $y^+ = 20$ is biased towards positive streamwise vorticity. As the wall phase increases, the direction of the bias flips and negative streamwise vorticity is preferred. This behavior is consistent with the model presented in Figure 2. While the distributions at $y^+ = 10$ and $y^+ = 30$ roughly follow the same behavior, a phase shift can be observed. We hypothesize that this phase shift is consistent with the phase shift induced by Stokes layer oscillations, and we have some preliminary data to support that. For example, a phase shift of approximately 90° from $y^+ = 10$ to 20 can be observed indicating that when the bottom of the vortices are strengthened, the tops show a decreased skewness. This indicates a warping of the vortex structure in which the legs of the hairpins are being strengthened on the bottom while remaining relatively unchanged at the top. As the vortical energy diffuses upwards we can see that the bias towards positive vorticity occurs at $y^+ = 20$.

If a fluid parcel traveling at roughly the root-mean square of the radial velocity fluctuations speed is considered ($\approx 0.1 - 0.4u_\tau$ between $10 < y^+ < 20$), traversing up

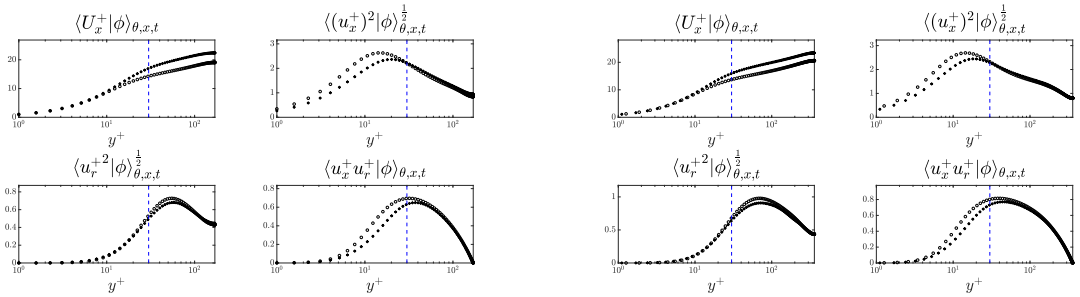

(a) Mean, RMS, and Reynolds Stress profiles for $Re_\tau = 170$ standard and drag reduced turbulent pipe flow

(b) Mean, RMS, and Reynolds Stress profiles for $Re_\tau = 360$ standard and drag reduced turbulent pipe flow

Figure 1: $\circ-$ standard pipe, $\star-$ oscillated pipe. RMS stands for "root-mean square". The blue line indicates the end of the buffer layer at $y^+ = 30$

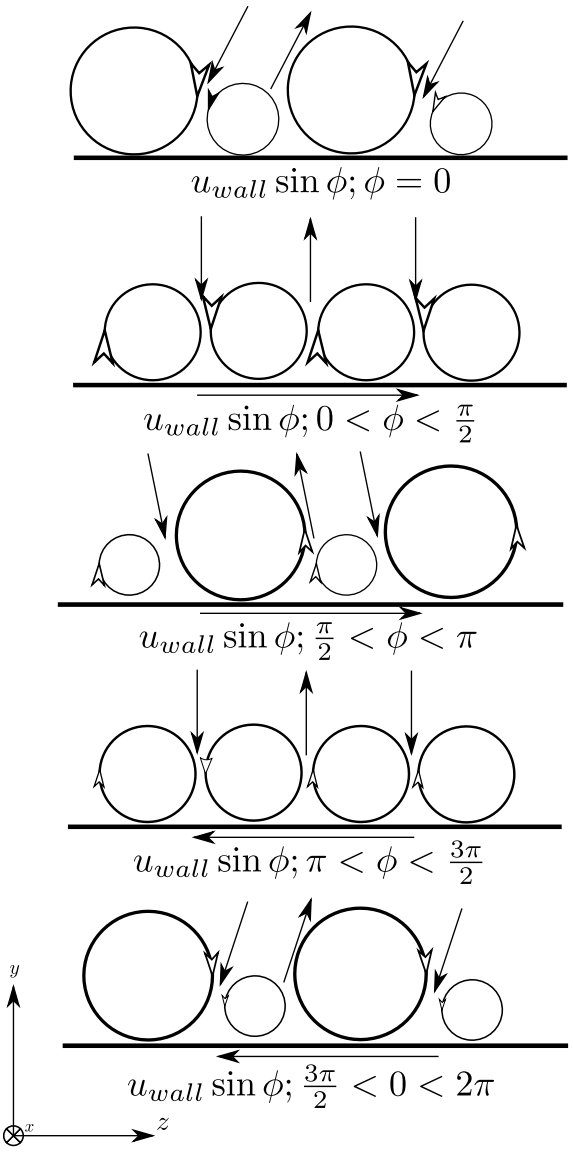

Figure 2: Model for effects of wall oscillations on quasi-streamwise vortices at various phase angles. Circles with hollow arrows indicate vorticity and its direction (clockwise positive, counter-clockwise negative looking from upstream down) and the black filled arrows indicate in-plane velocity fluctuations.

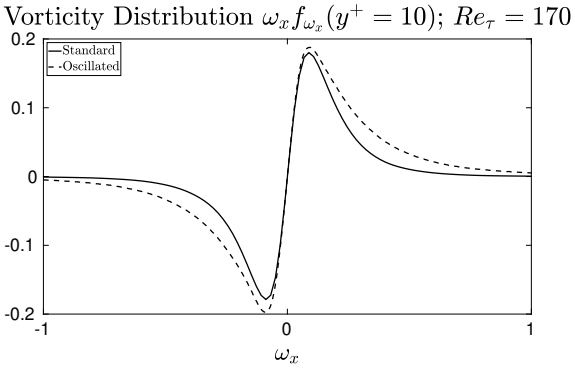

Figure 3: Pre-multiplied distribution of streamwise vorticity for $Re_\tau = 170, y^+ = 10$. This location sits roughly at the base of the streamwise vortices

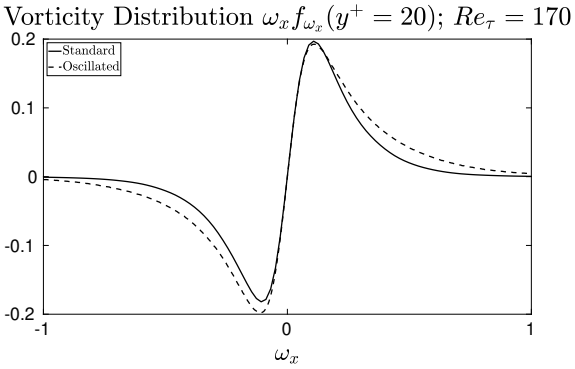

Figure 4: Pre-multiplied distribution of streamwise vorticity for $Re_\tau = 170, y^+ = 20$. This location sits roughly at the top of the streamwise vortices.

a vortex tube by induction, then a simple order of magnitude estimate implies that it will take roughly 40 time units ($t^+ \sim 10/.25 = 40$) to move from the bottom to the top of the vortex. This is equivalent to 144° of wall phase angle which is about half of the full wall oscillation period. According to Figure 2, over the half an oscillation period, a vortex undergoes a full cycle of being in its most energetic stage to a most weakened stage. Thus, by the time an energized particle from the bottom reaches the top, the vortex has lost almost all of its energy. The particle then has a lesser probability of being entrained into an ejection, and

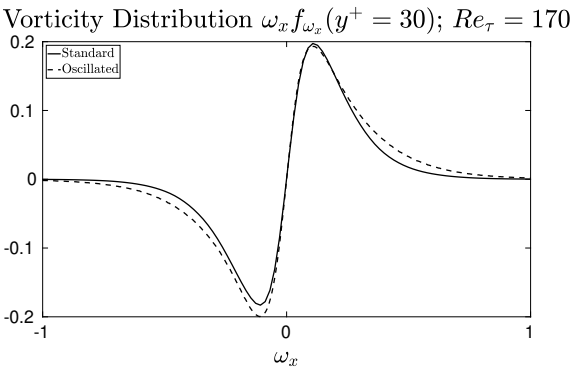

Figure 5: Pre-multiplied distribution of streamwise vorticity for $Re_\tau = 170, y^+ = 30$.

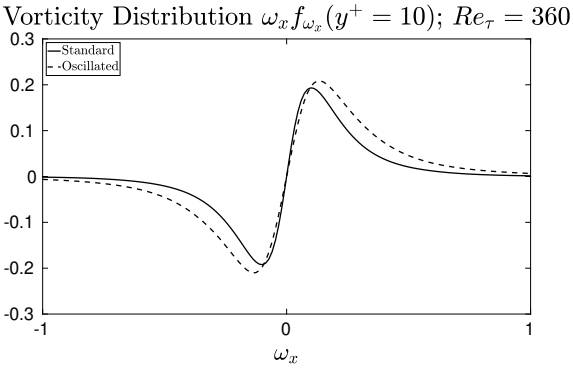

Figure 6: Pre-multiplied distribution of streamwise vorticity for $Re_\tau = 360$ at $y^+ = 10$

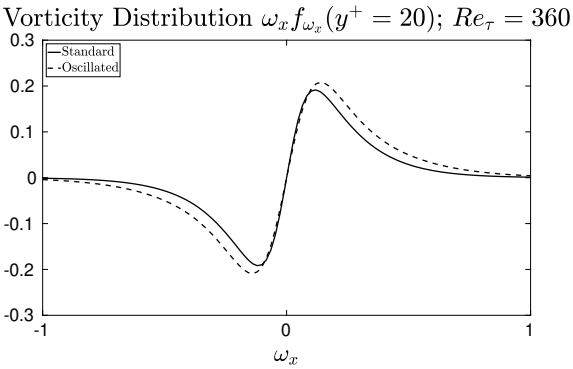

Figure 7: Pre-multiplied distribution of streamwise vorticity for $Re_\tau = 360$ at $y^+ = 20$.

Table 1: Tablulated Variance of Streamwise Vorticity

	$Re_\tau = 170$	$Re_\tau = 360$
y^+	OSC/STD	OSC/STD
10	2.237	2.114
20	1.694	1.630
30	1.406	1.357
44	1.219	1.216

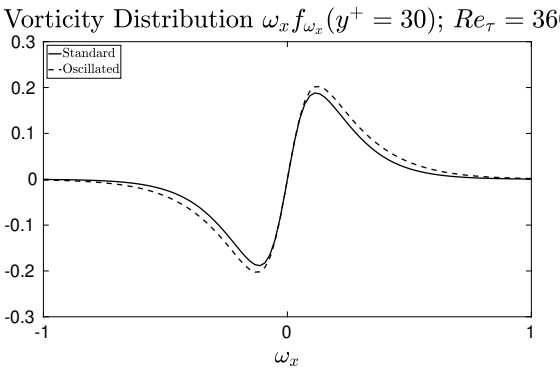

Figure 8: Pre-multiplied distribution of streamwise vorticity for $Re_\tau = 360$ at $y^+ = 30$.

will continue moving in a tangential direction. The net effect would appear to keep a fluid parcel "in orbit" with the vortex resulting in the observed transverse velocity.

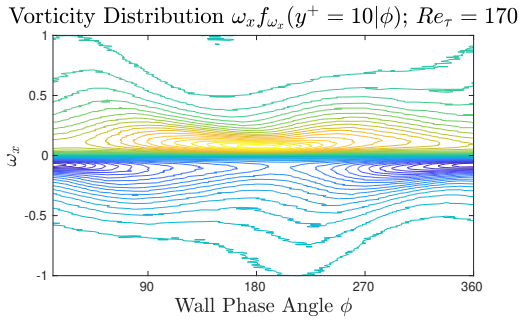

Figure 9: $Re_\tau = 170$ wall phase dependent streamwise vorticity distribution at $y^+ = 10$

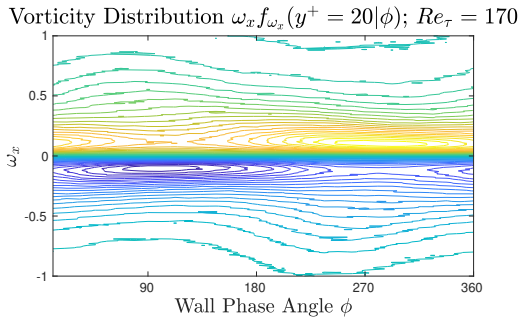

Figure 10: $Re_\tau = 170$ wall phase dependent streamwise vorticity distribution at $y^+ = 20$

To better visualize the phase shift between different y^+ locations, we compare the expected values of positive streamwise vorticity at $y^+ = 10, 20$ and 30 coordinates. To estimate the expected value of positive vorticity, we perform an integration of the form $\frac{1}{\sigma_{\omega_x}} \int_0^{+\sqrt{\sigma_{\omega_x}}} \omega_x f_{\omega_x} d\omega_x$ for each wall phase angle, where σ_{ω_x} is the variance (phase angle dependent). Figures 15 and 16 illustrate the variation along with the phase of wall oscillation for different y^+ values. The phase delay, as measured, follows the phase shift as a

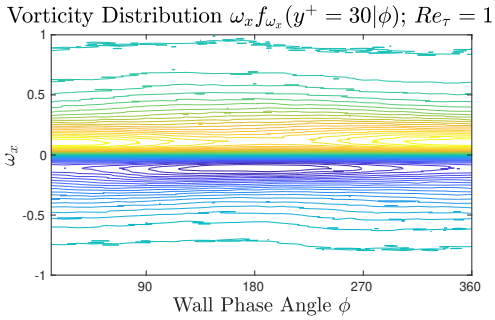

Figure 11: $Re_\tau = 170$ wall phase dependent streamwise vorticity distribution at $y^+ = 30$

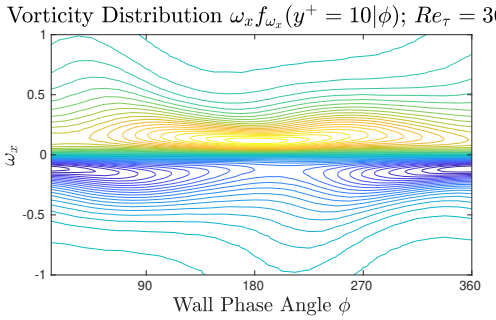

Figure 12: $Re_\tau = 360$ wall phase dependent streamwise vorticity distribution at $y^+ = 10$

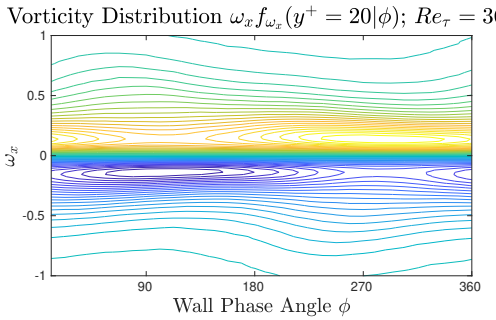

Figure 13: $Re_\tau = 360$ wall phase dependent streamwise vorticity distribution at $y^+ = 20$

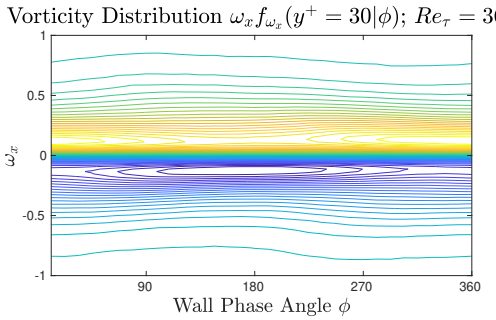

Figure 14: $Re_\tau = 360$ wall phase dependent streamwise vorticity distribution at $y^+ = 30$

result of the Stokes layer. The phase shift due to the Stokes layer between the wall locations separated by Δy^+ is analytically given by $\Delta\phi = \sqrt{\frac{\pi}{T^+}}\Delta y^+$. For the wall distance separation $\Delta y^+ = 10$ between $y^+ = 10$ and 20, this value results in $\Delta\phi = \sqrt{\frac{\pi}{100}}10 \sim 1.77$ corresponding to $\sim 101°$. From the Figures 15 and 16, the peak for $y^+ = 10$ occurs at roughly 180°, the peak at $y^+ = 20$ occurs at approximately 280°, and the peak at $y^+ = 30$ occurs at approximately 360°, giving the phase difference of about 100° for all three wall locations for both Reynolds numbers. Another observation from Figures 15, 16 is that the overall value of the expected one-sided vorticity reduces with the distance from the wall, showing that the skewing effect is stronger for the bottom portion of the vortices.

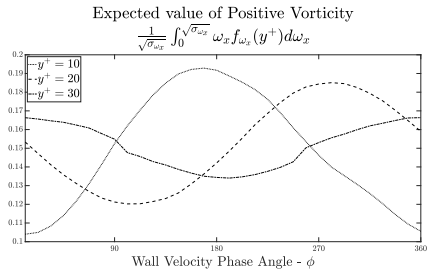

Figure 15: Expected Value of Positive Vorticity normalized by the RMS at $y^+ = 10, 20, 30$ for $Re_\tau = 170$

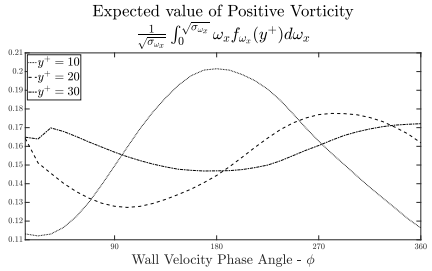

Figure 16: Expected Value of Positive Vorticity normalized by the RMS at $y^+ = 10, 20, 30$ for $Re_\tau = 360$

The implications are that the tops of the vortices are being strengthened less and at a later time than the bottom. This results in further skewing of the vortex tubes not only in relative size to one another, but also from the top to the bottom within the vortex tube.

6 Phase Variation of Velocity Fluctuations

From the Bio-Savart law, it follows that if the vorticity is alter, the induced velocity ought to be altered as well, including azimuthal and radial velocity fluctuaitons. Figures 17 through 20 show the behavior of the distribution of radial and transverse velocity fluctuations at $y^+ = 10$.

It can be seen that as the magnitude of the azimuthal fluctuations increase, the radial fluctuations decrease. This comes as a result of the vortices inducing an azimuthal velocity leading to a momentum transfer in the azimuthal rather than radial direction. This transfer along constant y^+ does not contribute to increasing the velocity gradient.

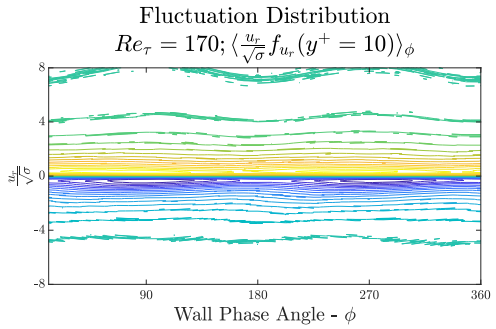

Figure 17: $Re_\tau = 170$ phase averaged distribution of radial velocity fluctuations at $y^+ = 10$

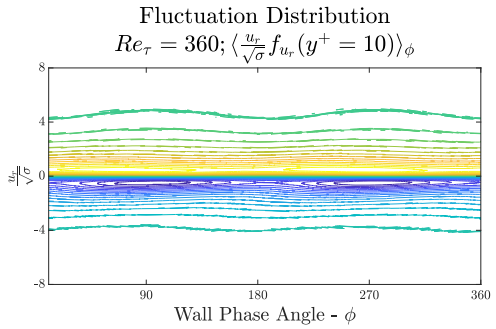

Figure 18: $Re_\tau = 360$ phase averaged distribution of radial velocity fluctuations at $y^+ = 10$

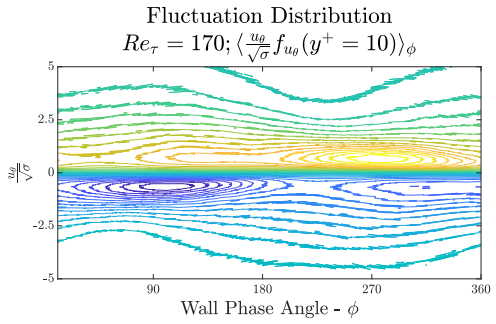

Figure 19: $Re_\tau = 170$ phase averaged distribution of azimuthal velocity fluctuations at $y^+ = 10$

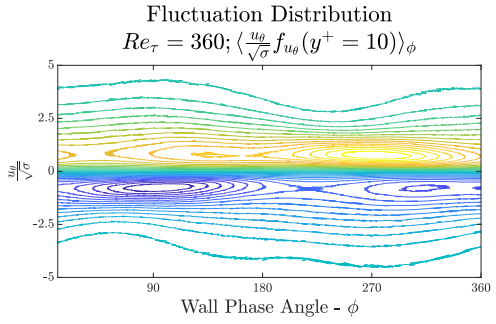

Figure 20: $Re_\tau = 360$ phase averaged distribution of azimuthal velocity fluctuations at $y^+ = 10$

7 Conclusions

Presented are the phase averaged distributions of vorticity in a drag reduced turbulent pipe flow with two different Reynolds numbers. The long term average distributions are compared to a standard pipe flow to observe long term changes in the streamwise vorticity variance. Phase distributions of vorticity, as well as azimuthal and radial velocity fluctuations are also presented. It is found that wall oscillations have the effect of increasing the likelihood of occurrence of large streamwise vortices in the region below the buffer layer. A phase to phase analysis of vorticity distributions shows a skewness of vorticity dependent upon the wall phase angle. This skewness in the distribution of vorticity results in a skewness in the induced velocity fluctuations in the radial-azimuthal plane. Based upon these findings we propose a heuristic model of effects of the wall oscillation on the near wall vortices. This model shows how the momentum transfer from the near wall to the log-layer is reduced by imposed transverse velocities resulting from unequal strength vortices and their interaction.

8 Acknowledgements

Support of NSF-CBET under the grant number 1707075 is highly acknowledged.

REFERENCES

Baron, A. & Quadrio, M. 1995 Turbulent drag reduction by spanwise wall oscillations. *Applied Scientific Research* pp. 311–326.

Choi, Jung-Il, Xu, Chun-Xiao & Sung, Hyung Jin 2002 Drag reduction by spanwise wall oscillation in wall-bounded turbulent flows. *AIAA journal* **40** (5), 842–850.

Choi, K. S. & Graham, M. 1998 Drag reduction of turbulent pipe flows by circular-wall oscillation. *Physics of Fluids* pp. 7–9.

Deville, M. O., Fischer, P. F. & Mund, E. H. 2002 *High-Order Methods for Incompressible Fluid FLow*. Cambridge University Press.

Duggleby, A., Ball, K. S. & Paul, M. R. 2007 The effect of spanwise wall oscillation on turbulent pipe flow structures resulting in drag reduction. *Physics of Fluids* pp. 1–12.

Fischer, P. 1997 An overlapping Schwarz method for spectral element solution of the incompressible Navier-Stokes equations. *J. Comp. Phys.* **133**, 84–101.

Guala, M., Hommema, S. & Adrian, R. 2006 Large-Scale and Very-Large-Scale motions in Turbulent Pipe Flow. *Journal of Fluid Mechanics* **554**, 521–542.

Hussain, Abul Khair Muhammad Fazle & Reynolds, William C 1970 The mechanics of an organized wave in turbulent shear flow. *Journal of Fluid Mechanics* **41** (2), 241–258.

Quadrio, M. & Ricco, P. 2004 Critical assessment of turbulent drag reduction through spanwise wall oscillations pp. 251–271.

Quadrio, Maurizio, Ricco, Pierre & Viotti, Claudio 2009 Streamwise-travelling waves of spanwise wall velocity for turbulent drag reduction. *Journal of Fluid Mechanics* **627**, 161–178.

Quadrio, M. & Sibilla, S. 2000 Numerical simulation of turbulent flow in a pipe oscillating around its axis. *Journal of Fluid Mechanics* pp. 217–241.

Zhou, D & Ball, Kenneth S 2008 Turbulent drag reduction by spanwise wall oscillations .